Analytical approximation to pion-nucleus scattering near the (3,3) resonance

Jean-Francois Germond
Institut de Physique, Neuchâtel, Switzerland

Mikkel B. Johnson
Los Alamos Scientific Laboratory, Los Alamos, New Mexico 87544
(Received 19 February 1980)

Starting from the eikonal approximation to the scattering amplitude an analytical approximation is obtained, including Coulomb effects. The amplitude is characterized by three numbers, one of which is a radius parameter b_1. These numbers are related in a simple way to the optical potential $U(r)$ for $r \simeq b_1$. The quality of the analytical result is assessed by comparing it to the exact eikonal amplitude for a model of U which is linear in density. It reproduces accurately the position and depth of the first minimum, the magnitude of the first secondary maximum, and the differences of the π^+ and π^- cross sections. It is furthermore shown that at 180 MeV the analytical approximation reproduces semiquantitatively the magnitude and shape of the "model exact" solution of the Klein-Gordon equation at forward angles. An application to scattering by the calcium isotopes is taken as an example to show the sensitivity to the neutron distribution as the $f_{7/2}$ shell is filled.

NUCLEAR REACTIONS Pion elastic scattering; analytical formulas for angular distributions.

I. INTRODUCTION

With the publication of the first high quality pion-carbon scattering data from CERN[1] the Glauber model (or equivalently the eikonal approximation) was shown to reproduce the general features of elastic and inelastic pion-nucleus scattering around the (3,3) resonance.[2,3] These calculations required as much computational effort as solving the Klein-Gordon equation, and shortly thereafter the optical model became more popular, especially because one could then go beyond the static limit.[3,4] Although optical model calculations remain the most flexible technique for calculating elastic scattering, eikonal techniques have an advantage, namely that they permit very simple interpretations of effect such as those due, for example, to the electromagnetic interaction.[5] In view of this, we return to the eikonal framework and look for an analytical solution which is both numerically accurate and more amenable to physical interpretation.

One such approximation scheme has recently been explored by Bethe and Johnson.[6] The result obtained there was very simple but it did not include the Coulomb effects and did not describe accurately the magnitude of the cross section at the position of the first secondary maximum. We attempt in the present work to remedy both deficiencies. The improvements are based on techniques developed by Frahn and Venter[7] to deal with situations in which there is strong absorption.

The practical value in pursuing this problem stems from the fact that today, with the advent of the high resolution pion spectrometers at LAMPF and SIN, accurate new data on heavy nuclei are becoming available in the energy region close to the first pion-nucleon resonance.[8,9] One of the primary hopes of these experiments is to take advantage of the strong π^--neutron interaction at these energies and extract information on the neutron distribution. The calcium isotopes are a particularly interesting case because extensive theoretical calculations of nuclear structure exist.[10-12] Also, ^{40}Ca is the heaviest $N = Z$ nucleus which allows the study of electromagnetic effects without large contributions from the neutron-proton density differences. In addition to the question of neutron distributions and Coulomb effects, there are also interesting questions to be resolved concerning the nature of the pion-nucleon interaction in the nuclear medium. Although our paper is pedagogical and no comparisons to data are made, we shall illustrate the theory with calculations on the calcium isotopes anticipating a subsequent detailed application to this data.

Section II recalls the main results of the eikonal formalism and discusses simple approximations to the phase function in impact parameter space. Frahn and Venter techniques[7] are then used to derive an analytical expression for the elastic scattering amplitude. In Sec. III the analytical results are compared to the exact eikonal theory in a model, which is the lowest order Laplacian theory. In Sec. IV the analytical theory is compared to the "model exact" solution of the Klein-Gordon equation with the lowest order Laplacian potential. In the conclusion, Sec. V, we consider

the limitations to our approach and generalizations to other channels.

II. DERIVATION OF FORMULAS

Using the eikonal formalism, the elastic scattering amplitude at momentum transfer q can be written as

$$F(q) = F_{pt}(q) + F_{CN}(q) , \qquad (2.1)$$

where F_{pt} represents the point Coulomb amplitude and

$$F_{CN}(q) = ik \int_0^\infty b\,db\,J_0(qb)e^{i\chi_{pt}(b)}\Gamma_{CN}(E:b) . \qquad (2.2)$$

In Eq. (2.2) k denotes the center of mass momentum of the incident pion, b the impact parameter, and Γ_{CN} the profile function. The separation (2.1) reflects only the additive Coulomb phase,[13] but there are other Coulomb effects coming from the distortion of the pion trajectory and from the energy dependence of the profile function. However, near the $(3,3)$ resonance pion scattering is very absorptive and these two effects reduce to trivial shifts as derived in Ref. 5:

$$\Gamma_{CN}(E:b) = 1 - \exp[i\chi_{CN}(E:b)] \qquad (2.3a)$$

$$= 1 - \exp[i\chi_N(E - V_c(b):b[1 + EV_c(b)/k^2])$$
$$+ i\chi_c(b) - i\chi_{pt}(b)] , \qquad (2.3b)$$

where the last term also takes account of the extension of the nuclear charge. The phase function χ_{CN} is related to the optical potential U by the usual integration along the average of the incident and outgoing pion momenta:

$$\chi_N(E:b) = -\frac{1}{2k} \int_{-\infty}^\infty dz\, U(E:(b^2 + z^2)^{1/2}) . \qquad (2.4)$$

In Ref. 6 a useful approximation for $\chi_{CN}(E:b)$ at large impact parameter was derived assuming that $U(r)$ is approximated by an exponential in the region of the nuclear surface near b.

$$\chi_{CN}(E:b) \simeq -(2\pi a_0 b)^{1/2}U(b)/2k , \qquad (2.5)$$

where a_0 is the distance over which $U(r)$ falls by $1/e$ of its value at b. Wallace[14] has given a prescription for improving the eikonal approximation so that it more nearly reproduces the solution of the corresponding "model exact" theory, which is the Klein-Gordon equation with the same U.

In order to obtain our analytical approximation we first perform an approximate integration by parts of Eq. (2.2) to write

$$F_{CN}(q) \simeq (1 + \eta^2/2)F_{CN}^{(1)}(q) + (1 - \tfrac{3}{2}i\eta)F_{CN}^{(2)}(q) \qquad (2.6)$$

with

$$F_{CN}^{(1)}(q) = \frac{-ik}{q} \int_0^\infty b\,db\,J_1(qb)e^{i\chi_c(b)}\Gamma_{CN}'(b) \qquad (2.7)$$

and

$$F_{CN}^{(2)}(q) = \frac{-2\eta k}{q^2} \int_0^\infty db[1 - J_0(qb)]e^{i\chi_c(b)}\Gamma_{CN}'(b) , \qquad (2.8)$$

where $\eta = Z\alpha E/k$ denotes the Coulomb parameter. Equations (2.6)–(2.8) are exact in second order in η for not too large values of the momentum transfer q. Only $F_{CN}^{(1)}$ survives when the Coulomb interaction is switched off. The additional term $F_{CN}^{(2)}$ added to F_{pt} represents the Coulomb scattering amplitude distorted by the strong interaction.

The quantity $\Gamma_{CN}'(b)$ maps out the domain probed in the scattering process. In the limit that $\Gamma_{CN}'(b)$ is a delta function we get the usual black disc scattering amplitude upon evaluating Eqs. (2.6)–(2.8). For the scattering of pions near the $(3,3)$ resonance the derivative of the profile function is sharply peaked (about the point $b = \bar{b}$) but it is essential to take into account its finite width; the important values of b are about 1 fm larger than the half-density radius, and at such a large impact parameter the nuclear density amounts to only 10% of its central value.[6] In this region of the nucleus, $U(b)$ is rapidly falling and we may characterize the phase χ_{CN} by its value $\chi_{CN}(b_1)$ at a point $b_1 \simeq \bar{b}$, and by its rate of change at the same point [see Eq. (2.5)]. We therefore define a diffuseness a,

$$a(b_1) = -\chi_{CN}(b_1)/\chi_{CN}'(b_1) \qquad (2.9)$$

and represent $\chi_{CN}(b)$ as[6]

$$\chi_{CN}(b) = \chi_{CN}(b_1)e^{(b_1 - b)/a(b_1)} . \qquad (2.10)$$

The location of the maximum is found by solving

$$\frac{d^2}{db^2}\Gamma_{CN}(\bar{b}) = 0 . \qquad (2.11)$$

Using the relationship in Eq. (2.10) we easily find the connection between b_1 and $\bar{b}$ to be

$$\bar{b} = b_1 + a(b_1)\ln[-i\chi_{CN}(b_1)] . \qquad (2.12)$$

We shall define b_1 to be the point at which

$$|\exp[i\chi_{CN}(b_1)]| = \tfrac{1}{2} , \qquad (2.13)$$

which coincides with the definition in Ref. 6. In this case Eq. (2.12) becomes

$$\bar{b} = b_1 + a(b_1)[\ln\ln 2 + \tfrac{1}{2}\ln(1 + \gamma^2) - i\arctan Y] , \qquad (2.14)$$

where

$$Y \equiv \operatorname{Re}\chi_{CN}(b_1)/\operatorname{Im}\chi_{CN}(b_1) . \qquad (2.15)$$

A straightforward calculation gives the full width at half maximum to be

$$\text{width of } \Gamma'_{CN} \approx 1.97 |a| . \tag{2.16}$$

For finite but small values of the diffuseness a, expansion techniques are useful for accurately evaluating Eqs. (2.6)–(2.8). A systematic procedure was developed many years ago by Frahn and Venter[7] in the case of profile functions *symmetric* around $\bar{b}$. In order to obtain the result we are seeking it is necessary to generalize their results to profile functions not symmetric around $\bar{b}$, such as the one generated by Eq. (2.10), and to include the Coulomb phase to lowest orders in $Z\alpha$.

To proceed, use is made of a Poisson-type integral representation for the Bessel functions $J_n(x)$ given by Eq. 7.3 (7) of Ref. 15. It expresses Eqs. (2.7) and (2.8) in terms of the "shifted" Fourier transforms of Γ'_{CN} defined by

$$G(x) \equiv \int_{-\infty}^{\infty} db\, e^{ix(b-\bar{b})} [-e^{i\chi_c(b)} \Gamma'_{CN}(b)] , \tag{2.17}$$

where $\bar{b}$ is defined in Eq. (2.14). By expanding $G(x)$ around $x = q$, the scattering amplitudes $F_{CN}^{(i)}$ can be expanded in a series of Bessel functions. Rearrangement of this series up to second order in the diffuseness a gives

$$F_{CN}^{(1)}(q) = ikR_+ \frac{J_1(qR_+)}{q} G_+(q) , \tag{2.18a}$$

$$F_{CN}^{(2)}(q) = \frac{2\eta k}{q^2} [G_+(0) - J_0(qR_-)G_+(q)] , \tag{2.18b}$$

where

$$G_+(q) = \tfrac{1}{2}[G(q) + G(-q)] \tag{2.19}$$

and

$$R_{\pm}^2 = \bar{b}^2 + \bar{b}\, \frac{G(q \mp i/2\bar{b}) - G(-q \mp i/2\bar{b})}{iqG_+(q)} . \tag{2.20}$$

At this point the only specific property of $\Gamma'_{CN}(b)$ used is that it is sharply peaked about $\bar{b}$. If we now use Eq. (2.10) we can obtain an analytic form for $G(q)$, defined in Eq. (2.14). Provided $\chi_c(b)$ is expanded around $\bar{b}$ it leads to

$$G(q) \simeq e^{i\chi_c(\bar{b})} \Gamma(1 - ia(q + 2\eta/\bar{b})) , \tag{2.21}$$

where $\Gamma(x)$ denotes the gamma (factorial) function.[16]

Equations (2.18)–(2.21) give an analytical expression for the scattering amplitude (2.1) including the effect of Coulomb. For a purely strong interaction the result is found to be of the fuzzy black disc type.[17] When Coulomb is included we find the usual Bethe phase[18] in front of $G(q)$, but there are also other Coulomb effects contained in R_+ and $F_{CN}^{(2)}$. The trajectory and energy shift

effects will manifest themselves through b_1, a, and Y and in the dependence of the scattering amplitude on them.

In the forward direction the scattering amplitude (2.2) with the approximate phase function (2.10) reduces to

$$F_{CN}(0) = \frac{ik}{2(1 + i\eta)} e^{i\chi_c(\bar{b})} \Gamma(1 - 2i\eta a/\bar{b})$$

$$\times \{ [\bar{b} - 2a\psi(1 - 2\eta i a/\bar{b})]^2$$

$$+ a^2 \psi'(1 - 2\eta ia/\bar{b}) \} , \tag{2.22}$$

where $\psi = \Gamma'/\Gamma$ denotes the digamma function.[16] The total cross section and relative real part is obtained by switching off the Coulomb interaction, i.e.,

$$\sigma_T = 2\pi \,\text{Re}\left[(\bar{b} + a\gamma)^2 + \frac{a^2\pi^2}{6} \right] , \tag{2.23a}$$

$$\frac{\text{Re}\, F_N(0)}{\text{Im}\, F_N(0)} = -\arg\left[(\bar{b} + a\gamma)^2 + \frac{a^2\pi^2}{6} \right] , \tag{2.23b}$$

where $\gamma = 0.5772$ is Euler's constant. In first order in the diffuseness a the expression (2.23) corresponds to the one obtained by Bethe and Johnson.[6] Its relative real part yields

$$\frac{\text{Re}\, F_N(0)}{\text{Im}\, F_N(0)} \simeq 2\, \frac{a}{b_1} \tan^{-1} Y , \tag{2.24}$$

and for small Y, this formula explicity shows that the real part comes from the edge of the black disk.

The complex zeros of the strong interaction amplitude $F_{CN}^{(1)}(q)$ defined by[4,19]

$$qR_+(q) = \text{zeros of the Bessel function } J_1 \tag{2.25}$$

contain in fact the same information as the forward amplitude because $R_+(q)$ is weakly dependent on the momentum transfer. To order a^3

$$R_+(q) = R_+(0) - 0.465\, a(aq)^2 \tag{2.26}$$

which shows that the black disk radius shrinks with increasing angle, but the variation is only of the order of a few percent at the position of the first minimum. Total cross sections and position of the first diffractive minimum determine the same quantity $\text{Re}\, R_+^2$ and do not allow the separation between the physical parameter b_1 and a. On the contrary, the rate of falloff for the maxima depends on the Inopin factor $G_+(q)$ and consequently on the diffuseness a. Differential cross section measurements up to the first secondary maximum are then required to determine unambiguously b_1, a, and Y.

III. COMPARISON OF APPROXIMATE AND EXACT EIKONAL THEORY IN A MODEL

In this section we wish to demonstrate that our analytical results are, in fact, accurate representations of the exact eikonal theory. We will not choose the most complicated interaction for this purpose, but we will make an attempt to pick one which has the features believed to dominate the physics of pion scattering in the (3, 3) resonance region. The Coulomb potential comes from a uniform charge distribution with radius R_c so that for impact parameters b larger than R_c, $V_c(R)$ reduces to the point Coulomb potential and $X_c - X_{pt}$ in Eq. (2.3b) vanishes. We choose the optical potential to be of the Laplacian form[3,20]

$$U(r) = -4\pi[b(r) + k^2 c(r) + \tfrac{1}{2}\nabla^2 c(r)] , \qquad (3.1a)$$

where

$$b(r) = b_0[\rho_n(r) + \rho_p(r)] - \epsilon_\pi b_1[\rho_n(r) - \rho_p(r)] , \qquad (3.1b)$$

$$c(r) = c_0[\rho_n(r) + \rho_p(r)] - \epsilon_\pi c_1[\rho_n(r) - \rho_p(r)] , \qquad (3.1c)$$

with ϵ_π the pion charge, and ρ_n and ρ_p the nuclear densities normalized to N and Z, respectively. The coefficients b_0, b_1, c_0, and c_1 are related to the free pion-nucleon interaction by

$$f_{\pi N} = b_0 + b_1 \vec{t} \cdot \vec{\tau} + (c_0 + c_1 \vec{t} \cdot \vec{\tau})k^2 \cos\theta , \qquad (3.2)$$

where the values of the parameters are taken from phase shift analysis.[21] The Laplacian form chosen in Eq. (3.1) is to leading order in density the result which would be obtained from the Kisslinger model. We do not consider the Wallace corrections in this section.

With this choice of model the real part of the derivative of the profile function is plotted in Fig. 1 for π^0-^{40}Ca elastic scattering at 180 MeV. Both proton and neutron density distributions have been represented by a Fermi distribution whose parameters were taken from electron scattering experiments,[22] i.e., $c_n = c_p = 3.51$ fm, $a_n = a_p = 0.517$ fm. The solid curve is the exact eikonal result, the short dashed curve is the approximation of Eq. (2.5), and the long dashed curve is the approximation of Eq. (2.10). The value of $\bar{b}$, defined earlier as the value of b at which the derivative of the profile function peaks, is seen to occur very near the point at which $|1 - \Gamma_{CN}| = \tfrac{1}{2}$, indicated by the arrow at $b \simeq 4.75$ fm in Fig. 1. It is seen in this figure that the approximations agree quite well with the exact calculation except for unimportantly small impact parameters. Away from the (3, 3) resonance the quality of approximation (2.10) in the model being discussed is still good, but the value of b_1 is smaller.
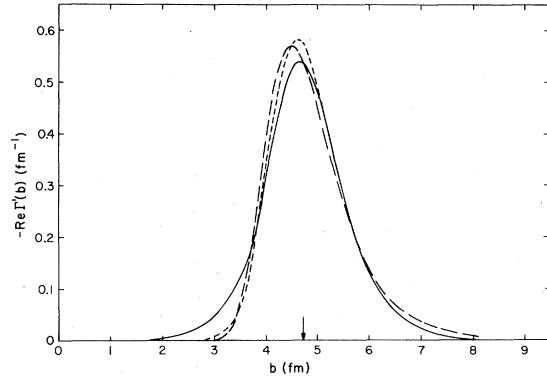
FIG. 1. Derivative of the profile function for π^0-^{40}Ca elastic scattering at 180 MeV. The solid curve results from the exact integration of Eq. (2.4), the dashed one from approximation (2.5), and the long dashed one from approximation (2.10).

In Fig. 2 we see the angular distributions for π^0-^{40}Ca scattering for three energies around 180 MeV in the same model. The solid curves represent the result of the exact eikonal approximation, whereas the dashed ones represent our analytical formula, Eqs. (2.18)-(2.21). The quantities b_1, a, and Y were obtained numerically [see Eqs. (2.9)-(2.15)] from an exact calculation of $\chi_{CN}(b)$. The agreement between these two curves is seen to be best at 180 MeV due to the small ratio a/b_1. The same comparisons are made in Fig. 3 for the relative π^-/π^+ differential cross sections. Note that Coulomb-nuclear interference effects in the minima are small at resonance[23] and the π^-/π^+ differences come from the Coulomb trajectory distortion and energy shift effects. In our analytical approximation these effects are all contained in the values of b_1, a, and Y.

To further check the validity of the analytical theory we shall investigate the extent to which it reproduces changes in the exact eikonal theory upon adding neutrons to the $f_{7/2}$ shell of calcium. Choosing ^{48}Ca as an example, we first take the shape of the nuclear density distribution to be the same as for ^{40}Ca except that the neutron half-density radius c_n is allowed to vary. Instead of looking at changes in the cross sections, it is easier and more transparent to look at changes in the relevant parameters contained in our analytical approximation.

Figure 4 shows the variations of b_1 at 180 MeV as a function of $\Delta c = c_n - c_p$, but only differences between values of b_1 are plotted. Curve (a) represents the difference between ^{48}Ca and ^{40}Ca for π^+, curve (b) the same for π^-, and curve (c) the differences between π^- and π^+ for ^{48}Ca. The solid curves result from the exact eikonal theory,
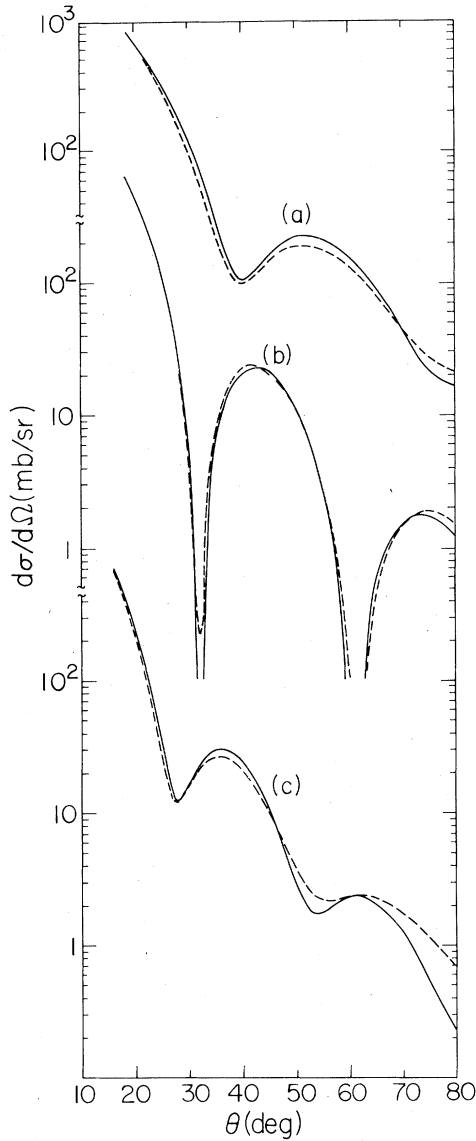
FIG. 2. Elastic differential cross sections for π^0-^{40}Ca at (a) 130, (b) 180, (c) 241 MeV incident pion energy. The solid curve corresponds to the eikonal approximation Eq. (2.2), and the dashed curve to our analytical approximation (2.18).

whereas the dashed ones have been obtained in the following way: we take only the isospin $\frac{3}{2}$ in the optical potential (3.1) and expand it in first order in Δc. This gives a relation between the phase function for ^{40}Ca and ^{48}Ca. Then using the approximate form (2.10) for χ_{CN} and the definition (2.13) of b_1 we find analytical relations which express Δb_1 in terms of quantities which appear in the optical potential.

The dashed curves in Figs. 4 (a) and 4 (b) correspond, respectively, to the expressions
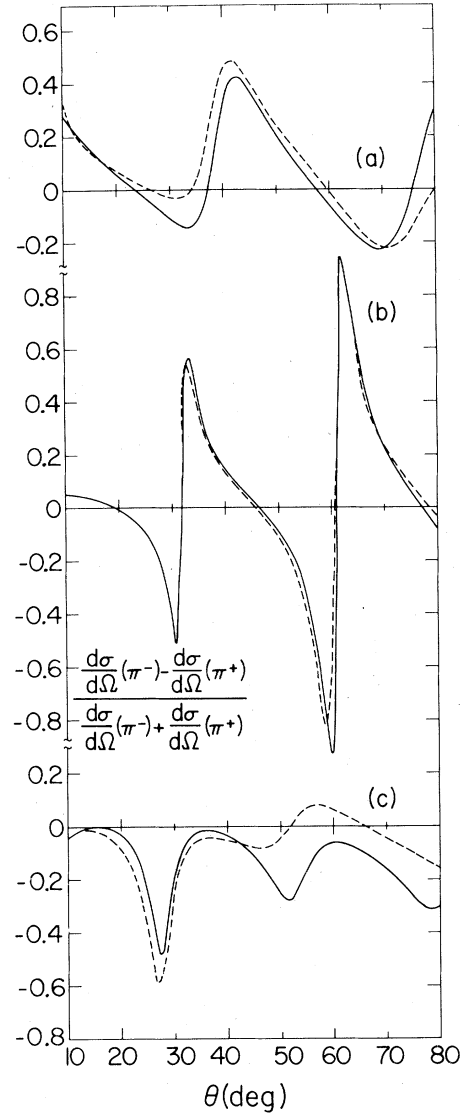
FIG. 3. Relative π^-/π^+ differential cross sections for pion scattering from ^{40}Ca at (a) 130, (b) 180, (c) 241 MeV incident pion energy. The legend is the same as for Fig. 2.

$$b_1^{48}(\pi^+) - b_1^{40}(\pi^+)$$

$$= a \ln\left(1 + \frac{1}{2A}\left[\Delta N + (\tfrac{1}{2}A + \Delta N)\frac{\partial b_1}{\partial c}\frac{\Delta c}{a}\right]\right) \quad (3.3a)$$

and

$$b_1^{48}(\pi^-) - b_1^{40}(\pi^-)$$

$$= a \ln\left\{1 + \frac{3}{2A}\left[\Delta N + (\tfrac{1}{2}A + \Delta N)\frac{\partial b_1}{\partial c}\frac{\Delta c}{a}\right]\right\},$$

$$(3.3b)$$

where $\Delta N = N - Z$ denotes the neutron excess and
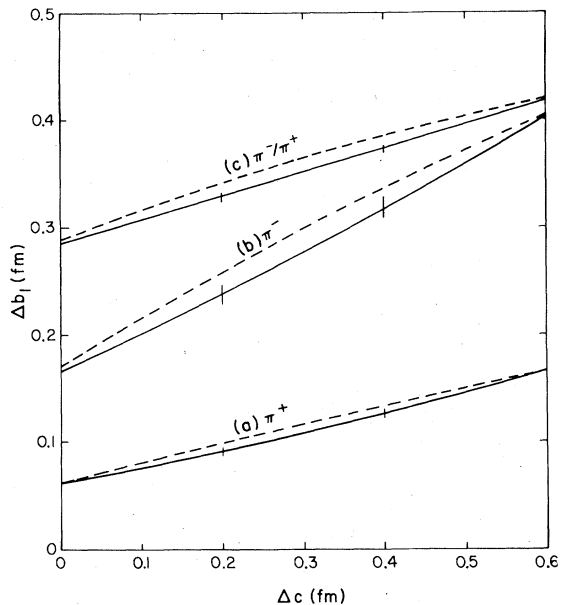
FIG. 4. Dependence of the critical impact parameter b_1 on the neutron half-density radius for pion scattering at 180 MeV: (a) difference between ^{48}Ca and ^{40}Ca for π^+, (b) the same for π^-, (c) difference between π^- and π^+ for ^{48}Ca. The solid curves are the results of the exact eikonal calculation whereas the dashed one is the approximations [(3.3)–(3.4)]. The error bars represent $\mp 20\%$ variation of the optical potential strength.

the other quantities refer to ^{40}Ca. At 180 MeV we have $a = 0.65$ fm and $\partial b_1/\partial c = 0.59$. Note that this latter quantity would be unity for a Fermi distribution, but is much smaller in our case which means that the sensitivity to Δc is also reduced. Equations (3.3) also show that the contribution of the neutron excess to Δb_1 (i.e., $\Delta c = 0$) is proportional to the diffuseness a. To minimize this term we must have a as small as possible and this happens just at resonance. But even there this contribution is about half of the total Δb_1 for $\Delta c = 0.3$. In general, however, we do not have a clean separation between the contribution of the neutron excess and the half radius difference.

The dashed curve in Fig. 4(c) for the π^-/π^+ difference is obtained by subtracting the two equations (3.3) and adding Coulomb effects. These effects are easily estimated in first order in the find structure coupling constant by substituting Eq. (2.3) into Eq. (2.10). The additional Coulomb effect Δb_1^c is

$$\Delta b_1^c = 2Z\alpha \frac{\partial}{\partial E} \ln k b_1 , \qquad (3.4)$$

which shows that Coulomb effects induce changes in b_1 only through the variation in energy of the

cutoff angular momentum $k b_1$. At 180 MeV, $(\partial/\partial E)\ln k b_1 = 0.61$ fm exactly reproduces the π^-/π^+ difference calculated for ^{40}Ca. Figure 4 confirms that our explicit approximations for Δb_1 are in fact very good, the discrepancies being always smaller than 0.025 fm.

IV. COMPARISON TO MODEL EXACT RESULTS

We have argued that our analytical approximation is capable of accurately reproducing the exact eikonal theory in the region of the (3,3) resonance. Because the eikonal amplitude can in principle be made to reproduce the "model exact" solution of the Klein-Gordon equation for the same U,[14] our result is established as a quantitative tool for studying pion-nucleus scattering in the (3,3) energy region. The remaining difficult question is to decide which theory for $\chi_{CN}(E:b)$ is the correct one for describing experimental results.

The contributions to $\chi_{CN}(E:b)$ may be divided into two distinct classes. The first consists of the terms which constitute U; this class describes the dynamics of the scattering process and has a well-defined density expansion[24] in terms of the underlying meson-nucleon interaction. All but the leading term, which is linear in the density, are difficult to calculate and are poorly understood. The second class consists of the Wallace corrections[14] which may also be arranged as an expansion in the density. These have been carefully studied and can be specified in terms of U.

It is generally assumed that the density expansion for $\chi_{CN}(E:b)$ (or U) converges, but there is no a priori reason why this should be true. However, as we have stressed, the important density for scattering in the vicinity of the (3,3) resonance is rather low density, and here the assumption of a rapidly convergent density expansion is plausible. It is essential to know which properties of the angular distribution are determined by this low density region of the nucleus and are therefore relatively insensitive to the addition of successively higher order terms in the optical potential. These properties are clearly the ones which should be the focus of attention in any meaningful attempt to compare theory to experimental data. We shall try to give at least a partial answer to this question here at the level of ρ^2 terms. Since there is no complete calculation of the dynamical ρ^2 contributions, we shall study the sensitivity of the theory to the first Wallace correction. This analysis will be applied to a calculation of π-calcium scattering at 180 MeV, as this corresponds to the recent data.[8,9]

We begin by showing in Fig. 5 a comparison between the eikonal π^0-^{40}Ca elastic scattering and the model exact computer calculation using the program PIRK.[25] Only the analytical eikonal theory is shown, as this compares favorably to the exact eikonal result [see Figs. 2(b) and 3(b)]. The long dashed curve is the model exact solution using the Laplacian potential defined in Eqs. (3.1a)–(3.1c). The dot-dashed curve is the analytical result with, and the short dashed curve the result without, the first Wallace correction.[14] In the former case, we modified (2.9) by U by

$$U + \frac{U^2}{4k^2}\left(1 + \frac{2b^2}{r}\frac{d}{dr}\ln U\right).\qquad(4.1)$$

Without the Wallace correction the approximate theory reproduces the magnitude of the model exact theory in the forward direction and at the secondary maximum. The location of the first minimum is reproduced, but the minimum is too deep in the approximate theory. The model exact and eikonal theories will differ substantially only away from resonance.[26] The addition of the Wallace correction improves the reproduction through the first minimum, but the height of the

secondary maximum is now overestimated by about 50%. Figure 6 shows a comparison between the π^-/π^+ differences. Again, the long dashed curve is the model exact solution. The results are obtained using a Coulomb energy shift of $Z\alpha/b_1$ in the input parameters. The short dashed curve is the result with no Wallace correction, and the large discrepancies are related to the fact that the depth of the minimum is not correctly reproduced without the Wallace correction. Note that at resonance the second term in Eq. (4.1) is real and will consequently generate π^+/π^- differences by interfering with the Coulomb potential. The dot-dashed curve includes the first Wallace correction, and there is now good agreement with the exact result throughout the forward direction.

The results in Figs. 5 and 6 show that the eikonal theory is a semiquantitative description of the model exact theory. However, the Wallace correction has a non-negligible effect on the extent of agreement, and we are led to ask which of the three quantities b_1, a, and Y are most accurately calculated.

We shall investigate this question by looking at the sensitivity of the angular distribution to the addition of neutrons in the $f_{7/2}$ shell. Our model of the density distribution in ^{48}Ca is the same as that discussed in Sec. III. We determine the pa-

FIG. 5. Elastic differential cross section for π^0-^{40}Ca at 180 MeV incident pion energy. The long dashes correspond to the Laplacian potential using PIRK. The short dashes correspond to our analytical approximation (2.18) with no Wallace correction. The dot-dashed curve is approximation (2.18) with the first Wallace correction.
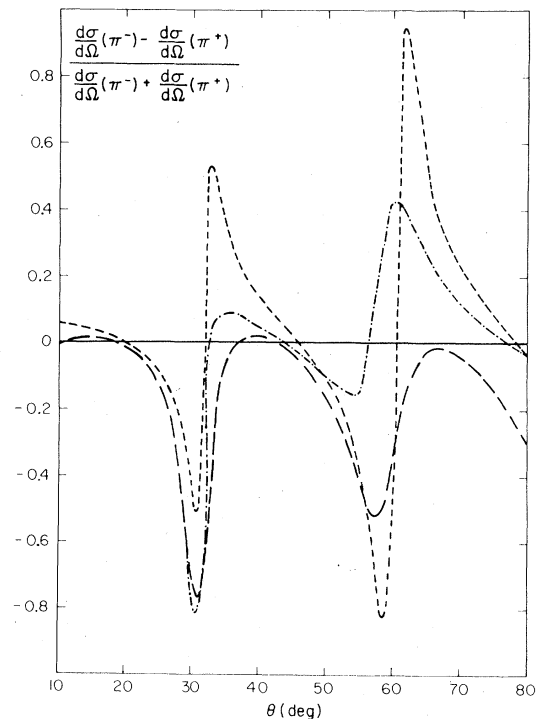
FIG. 6. Relative π^-/π^+ differential cross sections for pion scattering from ^{40}Ca at 180 MeV incident pion energy. The legend is the same as for Fig. 5.

rameters b_1, a, and Y by fitting our analytical
results to the position and depth of the first min-
imum and the magnitude of the secondary maxi-
mum, taking a to be purely real. The results of
this are shown in Table I. The density parameters
for the Woods-Saxon shape are $c_n = 3.81$, $c_p = 3.51$,
$a = 0.517$, which give a root mean square radius
difference between neutrons and protons of 0.2
fm, corresponding approximately to the same
quantity in the theory of Ref. 27. The magnitude of
b_1 agrees with the exact calculation extremely
well, whether or not the Wallace correction is
included. The maximum discrepancy in b_1 is less
than 3%. However, the ratio Y and diffuseness
a are sensitive to whether or not the Wallace
correction is included. Because Y is accurately
calculated when the Wallace correction is added,
the depth of the first minimum is probably not
very sensitive to ρ^3 and higher order terms. How-
ever, a is not accurately calculated at order ρ^2
and the addition of yet higher order effects are
probably required for a complete understanding
of this parameter.

We conclude from the above comparison that
the analysis of experimental data at 180 MeV
should be most concerned with the b_1 and Y pa-
rameters, and that there is some hope of under-
standing the systematics at the level of corrections
of orders ρ and ρ^2. One of the interesting ques-
tions is to understand how b_1 varies for fixed Z
as a function of N. In such an analysis we are
concerned with differences between theoretical
and experimental quantities, as some systematic
uncertainties tend to cancel when viewed in this
way. We therefore shown in Fig. 7 the differences
of the b_1 values in the three different calculations
of Table I. It is seen that the differences in the
b_1 values for π^- scattering agree very well, to
within 15%. There is a somewhat better agreement
for π^+. The Wallace correction does not affect
this comparison at 190 MeV, but at somewhat
lower or higher energies this correction is needed.
To understand the π^-/π^+ differences the Wallace
correction is required at 180 MeV because of
Coulomb effects.

It is natural to ask how sensitive the calculation
is to the parameters of the optical potential. We
thus recalculated the Δb_1's with the optical po-
tential renormalized by ±20%. We found a maxi-

mum variation of 0.01 fm, corresponding to a
change in angle of about 0.1°, which is approxi-
mately the accuracy of the present data.[8,9] The
actual variation is shown by the vertical errors
shown in Fig. 4.

V. CONCLUSIONS AND OUTLOOK

In this work we have studied the elastic scat-
tering of pions by nuclei in an energy domain
close to the first pion-nucleon resonance. Starting
from the eikonal approximation we derived in Sec.
II an analytical approximation for the scattering
amplitude of the "fuzzy black disc" type. In con-
trast to Ref. 28 our approximation is valid for
small momentum transfer only. The scattering
amplitude is characterized by three numbers, one
of which is a radius parameter b_1. All three num-
bers are related to the optical potential by simple
but accurate formulas.

In order to apply our results, the optical po-
tential must have a local representation. Thus,
the familiar Kisslinger and Laplacian models for
pion-nucleus scattering can be encompassed
within the framework of this approach. (To apply
the results to the Kisslinger theory a transfor-
mation must be made.[6]) As an example, we con-
sidered pion scattering by the calcium isotopes
using a first order Laplacian theory, but a wide
class of currently popular theories have a form
suitable for study within the context of this
approach (see, for example, Ref. 20). The eikonal
theory does not usefully apply to nonlocal po-
tentials, although in the resonance region at least
some of the effects of the finite range of the pion-
nucleon form factor can be accommodated by a
local interaction.[29] The severity of the limitation
to local potentials has not been carefully explored
and deserves further study.

One goal of medium energy pion physics is to
develop the possibility of using the pion as a probe
of nuclear structure. The variation of the pa-
rameter b_1 throughout an isotopic multiplet reflects
the changes in density as a result of adding valence
neutrons. We have carefully examined the adequacy
of the analytical theory to describe the behavior
of b_1 in a model and we found that it reproduces
$b_1({}^{48}\text{Ca}, \pi^\pm) - b_1({}^{40}\text{Ca}, \pi^\pm)$ to an accuracy of less
than 15%. We conclude that the analytical theory

TABLE I. Comparison of model exact problem to eikonal theory for $\pi^\pm$ ^{48}Ca at 180 MeV.

	$b_1^{(+)}$	$a^{(+)}$	$Y^{(+)}$	$b_1^{(-)}$	$a^{(-)}$	$Y^{(-)}$
Model exact	4.78	0.640	−0.388	4.96	0.666	−0.757
With Wallace	4.82	0.492	−0.392	5.02	0.491	−0.795
No Wallace	4.75	0.627	+0.106	5.10	0.612	−0.089
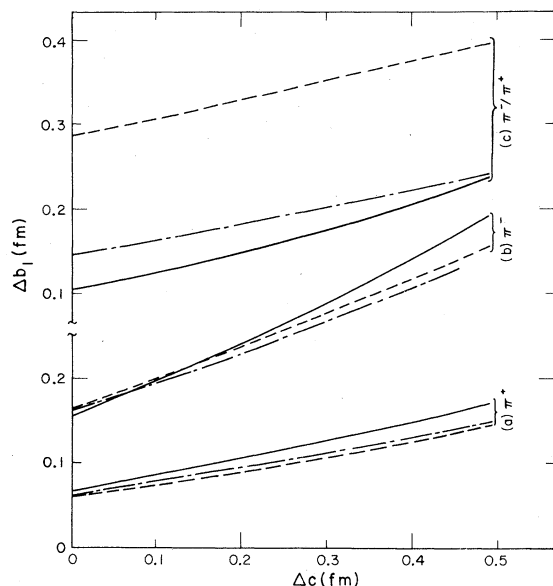
FIG. 7. Comparison of b_1 differences in model exact and eikonal theories for pion scattering at 180 MeV: (a) difference between ^{48}Ca and ^{40}Ca for π^+, (b) the same for π^-, (c) difference between π^- and π^+ for ^{48}Ca. The solid curves correspond to the Laplacian potential using PIRK, the dashed ones to our analytical approximation (2.18) without Wallace correction, the dot-dashed curve with the first Wallace correction.

is sufficiently accurate to draw quantitative conclusions from an application to experimental data.

Recently the use of pions to study the neutron halo was critized in Ref. 31. There it was found that the density distributions and parameters which determine the pion-nucleon amplitude in the optical potential were so strongly correlated that a unique characterization of the neutron distribution could not be obtained. However, in Ref. 31 different pion-nucleon scattering amplitudes were used in ^{40}Ca and ^{48}Ca. The relationship we have found between Δb_1 and the parameters of the density distribution [see, e.g. Eq. (3.3)] follow because we assumed that the $same$ U applies for scattering from ^{48}Ca and ^{40}Ca. There is no evidence that U should be chosen differently in these cases.

Two categories of corrections to the lowest order picture which we have studied here deserve

mention. One is charge symmetry breaking effects at the pion-nucleon level and the other is terms in the optical potential which are quadratic (or higher order) in the nuclear density. Using the measurements of $\pi^\pm$-d total cross sections[30] to estimate the charge symmetry breaking effects would result in an increase in Δb_1 for π^-/π^+ differences, as shown in Ref. 5. Very little is known about the higher order contributions to the optical potential. The variation of Δb_1 is most sensitive to the corrections to the isovector and isotensor pieces of the interaction, which are probed in charge exchange reactions. In any case, our approach is sufficiently flexible to permit the study of these effects as models are developed.

Our techniques could easily be extended to pion inelastic scattering to low lying excited states. This problem is interesting in the sense that the transition profile function will be peaked at different values of the impact parameter depending on the pion charge. Consequently π^+ and π^- will probe the neutron and proton transition densities at impact parameters a few tenths of a fermi apart. This could maks other effects such as Pauli blocking which were advocated to explain the 3^- data on the calcium isotopes.[9] Another application of our formalism concerns the single and double charge exchange to the analog states.[32] The results derived in the present paper would lead to more accurate angular distributions than the analytical results given in Ref. 32. More data especially on the calcium and tin isotopes are promised[33] at resonance where our analytical approximations work very well for elastic scattering. Any detailed analysis should then take into account all the channels, which our formulation can do easily.

[1]F. Binon et $al.$, Nucl. Phys. B17, 168 (1970); B33, 42 (1971); B40, 608 (1972).

[2]C. Schmit, Nuovo Cimento Lett. 4, 459 (1970); C. Wilkin, $ibid.$ 4, 491 (1970).

[3]For a general review on pion-nucleus scattering, see R. H. Landau, in $High$ $Energy$ $Physics$ and $Nuclear$ $Structure$, edited by D. F. Measday and A. W. Thomas (North-Holland, 1980), p. 289.

[4]J. P. Maillet, J. P. Dedonder, and C. Schmit, Nucl. Phys. 316, 267 (1979).

[5]J.-F. Germond and C. Wilkin, Ann. Phys. (N.Y.) 121, 285 (1979).

[6]M. B. Johnson and H. A. Bethe, Comments Nucl. Part. Phys. 8, 75 (1978); Los Alamos Report No. LA-76-1844 (1976).

[7]W. E. Frahn and R. J. Venter, Ann. Phys. (N.Y.) 24, 243 (1963); R. M. Venter, ibid. 25, 405 (1963).

[8]J.-P. Egger et al., Phys. Rev. Lett. 39, 1608 (1977); P. Gretillat, thesis, Univ. of Neuchâtel (unpublished).

[9]K. G. Boyer et al., Meson-Nuclear Physics—1979 (Houston) Proceedings of the 2nd International Topical Conference on Meson-Nuclear Physics, edited by E. V. Hungerford III (A. I. P. , New York, 1979), p. 529; C. L. Morris, private communication of EPICS Expt. No. 9 preliminary data.

[10]J. W. Negele, Phys. Rev. C 1, 1260 (1969); 9, 1054 (1974).

[11]M. Beiner et al., Nucl. Phys. A238, 29 (1975); Ann. Phys. (N.Y.) 86, 262 (1974).

[12]For a general review see J. W. Negele, in Proceedings of the LAMPF Workshop on Pion Single Charge Exchange, edited by H. Baer, D. Bowman, and M. B. Johnson, Los Alamos Report No. LA-7892-C, 1979, p. 250.

[13]R. T. Glauber, Lectures in Theoretical Physics (Interscience, New York, 1959), Vol. I, p. 315.

[14]S. J. Wallace, Ann. Phys. (N.Y.) 78, 190 (1973).

[15]A. Erdelyi, Higher Transcendental Functions (McGraw-Hill, New York, 1953), Vol. II.

[16]M. Abramowitz and I. A. Stegun, Handbook of Mathematical Functions (Dover, New York, 1970).

[17]E. V. Inopin and Yu. A. Berezhnoy, Nucl. Phys. 63, 689 (1965).

[18]H. A. Bethe, Ann. Phys. (N.Y.) 3, 190 (1958); M. M. Islam, Lectures in Theoretical Physica (Gordon and Breach, New York, 1968), Vol. XB, p. 97; M. D. Cooper, M. B. Johnson, and G. B. West, Nucl. Phys. A292, 350 (1977).

[19]A. Gersten, Nucl. Phys. B12, 537 (1969); A219, 317 (1974).

[20]K. Stricker, H. McManus, and J. Carr, Phys. Rev. C 19, 929 (1979), and references therein.

[21]G. Rowe, M. Salomon, and R. H. Landau, Phys. Rev. C 18, 584 (1978).

[22]At. Data and Nucl. Data Tables 14, 479 (1974).

[23]J.-F. Germond and C. Wilkin, Phys. Lett. 68B, 229 (1977).

[24]C. B. Dover, J. Hüfner, and R. H. Lemmer, Ann. Phys. (N.Y.) 66, 248 (1971).

[25]R. A. Eisenstein and G. A. Miller, Comp. Phys. Comm. 8, 130 (1974).

[26]J.-F. Germond and J.-P. Amiet, Nucl. Phys. A216, 157 (1973).

[27]J. W. Negele and D. Vautherin, Phys. Rev. C 5, 1472 (1972); 11, 1031 (1975).

[28]R. E. Amado, J.-P. Dedonder, and F. Lenz, SIN Report No. 7908 (1979).

[29]M. B. Johnson and D. J. Ernst, Phys. Rev. C 20, 1064 (1979).

[30]E. Pedroni, K. Gabathuler, J. J. Domingo, W. Hirt, P. Schwaller, J. Arvieux, C. H. Q. Ingram, P. Gretillat, J. Piffaretti, N. W. Tanner, and C. Wilkin, Nucl. Phys. A300, 321 (1978).

[31]M. M. Sternheim and K.-B. Yoo, Phys. Rev. Lett. 41, 1781 (1978).

[32]M. B. Johnson, Phys. Rev. C 22, 192 (1980).

[33]H. Baer et al. (unpublished).